LA-UR -85-1610

TITLE   CW OPERATION OF THE FMIT RFQ ACCELERATOR

AUTHOR(S)   W. D. Cornelius

DISCLAIMER

Los Alamos

Los Alamos National Laboratory
Los Alamos, New Mexico 87545

CW OPERATION OF THE FMIT RFQ ACCELERATOR[*]

W. D. Cornelius, AT-4, MS H821
Los Alamos National Laboratory, Los Alamos, NM 87545 USA

Summary

Recently, we have achieved reliable cw operation of the Fusion Materials Irradiation Test (FMIT) radio-frequency quadrupole (RFQ) accelerator. In addition to the operational experiences in achieving this status, some of the modifications of the vacuum system, cooling system, and rf structure are discussed. Preliminary beam-characterization results are presented.

Introduction

The FMIT accelerator was designed for the testing of materials to determine their suitability as first-wall materials in the high neutron-flux environment of fusion power reactors. The primary components of the FMIT system were a 35-MeV, 100-mA cw deuterium ion accelerator and a liquid lithium target. The development program for the prototype accelerator was divided into two stages. The first stage (2 MeV) involved the development of an injector and RFQ accelerator with output characteristics suitable for injection into a drift-tube linear accelerator (DTL). The second stage involved the addition of a DTL for subsequent acceleration to an energy of 5 MeV.

Background

We are now involved in the 2-MeV development program and have accelerated 20 mA cw of H_2^+ ion beam in the FMIT RFQ. The RFQ consists of two coupled, coaxial resonators (Fig. 1). The rf power is loop coupled into the outer section, or manifold, which uniformly distributes this power through the coupling slots into the inner resonator, or core. Achieving cw rf operation of the RFQ proved to be the most difficult part of the development and involved some modest modification of the RFQ structure.[1] Many effects that can be neglected at low duty factor become major considerations in a cw accelerator.

Surface outgassing, for example, can be extreme with the higher surface temperatures of cw structures (~200°C in some locations in the FMIT RFQ). The design of the FMIT RFQ prevented high-temperature vacuum bake-out, so the rf was used to heat the structure. The resulting hydrogen gas load caused high vacuum pressures (~10^{-5} torr) and thermal runaway of the ion pumps.

We have found cryopumps to be a good solution for our system. Not only do they outperform ion pumps with the same throat diameter, but the extra-large hydrogen capacity of the modern cryopumps provides a reasonably long time between regeneration cycles.

Thermal loading of surfaces and thermal stresses are the major problems when operating in a cw mode. Even with adequate cooling, the thermal gradients between the water-cooling channels and the rf surfaces can produce surface temperatures in excess of 150°C, as well as significant thermal stresses caused by differential expansion. Thermal expansion in the FMIT RFQ decreases the operating frequency by 170 kHz from start up to full-power operation. Thermal stresses were directly responsible for most of the problems encountered while attempting to achieve cw rf operation.[1] We solved most of these thermal problems by attaching additional water-cooling lines to those structures cooled only through thermal contact with other directly cooled regions and by accommodating thermal expansion in other areas such as the rf joints and end-wall closures.

In addition to thermal stresses and vacuum pumping, the only other major limitation to achieving cw operation was multipactoring in the manifold.[1] The initial disassembly of the RFQ in November 1983 revealed two dark, discolored bands around the structure near each coupling slot and evidence of multipactoring in other areas as well. Traditional methods to combat multipactoring have concentrated on coating the rf surfaces with a thin layer of titanium nitride (TiN) to lower the secondary-electron emission coefficient below unity.[2] In our experience, the durability of the surface coatings produced by previous techniques was
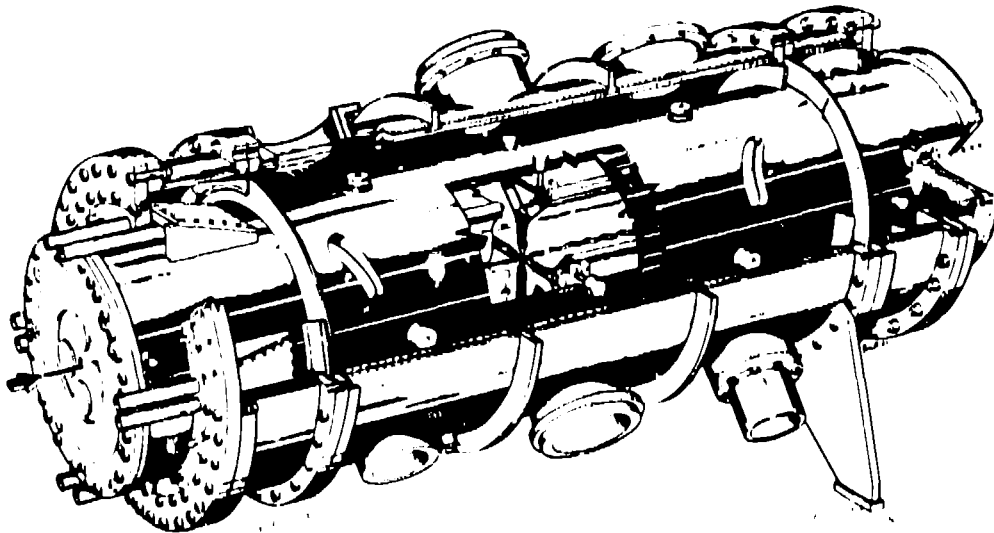

Fig. 1. Initial design of the FMIT RFQ accelerator. The RFQ comprises two coupled, coaxial resonators. The rf power is loop coupled into the outer section, or manifold, which more uniformly distributes the power into the four quadrants of the inner resonator, or core. A 75-keV beam is injected (arrow, left in the figure) and accelerated to 2 MeV.

poor, as was the long-term stability of the coating. However, we were able to modify this method slightly and have achieved an extremely durable surface coating with impressive results.[8] We have not observed any substantial evidence of multipactoring after coating the RFQ surfaces with a thin layer of TiN. There is also evidence that, as expected,[4] the outgassing rate of the copper rf surfaces has been reduced substantially.

With these modifications and a few other minor changes,[1] we were able to achieve full-power cw rf operation early in August 1984, and accelerated the first cw beam that same day. Except for a brief shutdown during November to eliminate the last thermal problem in the RFQ,[1] we have had few problems with cw operation. The RFQ is relatively easy to bring to full power. The time needed from a cold start can be as short as 30 min, but we usually take about an hour to minimize thermal-shock effects. This time complements nicely the time needed to bring the injector to stable operation. Hence, we can have cw 2-MeV beam on the beamstop within an hour of a cold start. Our recent problems have been due to beam-induced heating and subsequent loss of vacuum in the high-energy beam transport (HEBT) section. The FMIT 2-MeV beam has been compared to the "light-saber" from the Star Wars movies, efficiently cutting anything that gets in the way.

Instrumentation

Because the beam power is so high, we must use noninterceptive diagnostic instrumentation. The diagnostic devices being used have been rather extensively described in the literature and will only be mentioned here. The transverse emittance is determined by tomographic reconstruction from beam profiles obtained at several different locations along the beamline.[5] If the transport matrices relating the profiles are known, then the beam emittance can be derived. The transverse beam profiles are obtained by digitizing the light-intensity profiles emitted by the ionized residual-gas atoms in the vacuum. Spatially preserving fiber optics are used to guide the light onto a linear array of light-sensitive diodes.[6] The typical resolution is 130-μm/channel, more than adequate for the tomographic techniques. A typical intensity profile is shown in Figure 2, and an emittance reconstruction from three such profiles is shown in Figure 3.

The 2-MeV beam current is derived from beamstop calorimetry and from an 80-MHz pulse-current monitor (Pearson Electronics, Inc., Palo Alto, California). These currents can be compared with the rf power loading. Beam transmission can be determined from the ratio of the 2-MeV beam current to the injected beam current. The current in the low-energy beam transport line (LEBT) is determined by calorimetry and by a dc current transductor.[7]
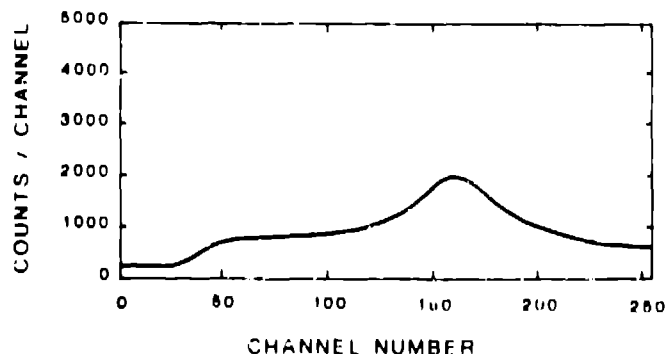
Fig. 2. Typical beam profile of the 2-MeV beam derived from the light emitted by the ionized residual gas atoms in the beampipe. The three contours plotted enclose 99.9%, 95%, and 65% of the beam.
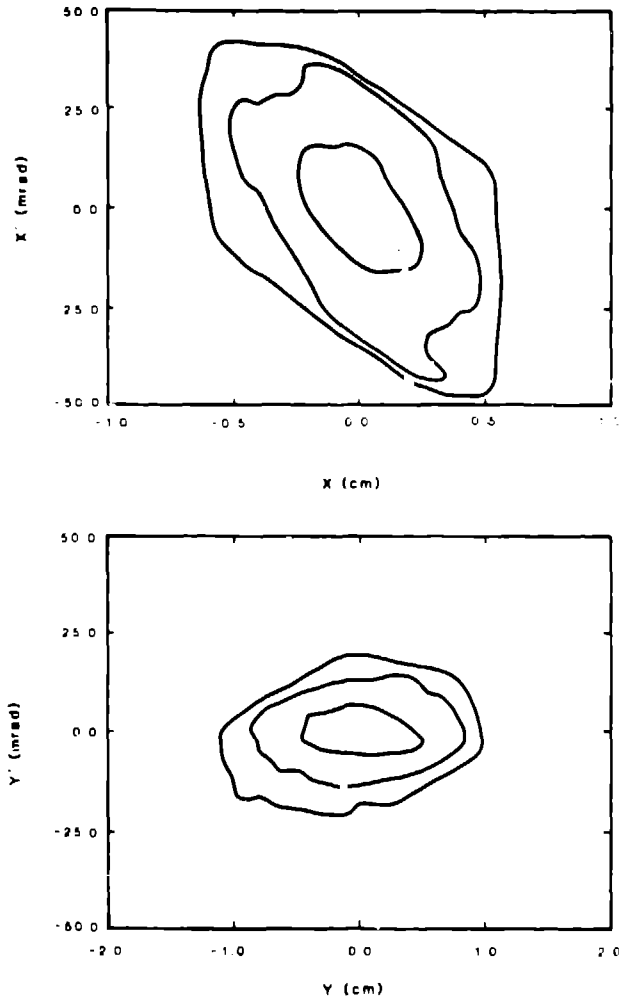
Fig. 3. Typical RFQ 2-MeV beam emittances derived by tomographic reconstruction from three beam profiles such as those shown in Fig. 2.

The beam energy and the longitudinal beam-profile can be derived, respectively, from the time of flight between two separated current loops (manufactured by NTG Nukleartehnick of West Germany) and from the Fourier transform of the signal from a single loop. The beam energy from the time loops compares favorably with values derived from magnetic deflection of the 2-MeV beam. The Fourier deconvolution of the longitudinal profile can, in principle, be compared with values derived from the time width of a gamma-ray peak produced by proton capture in a lithium target. These latter measurements are still in progress.

Results

The RFQ beam energy was easily confirmed to be 2 MeV as designed. The other measurements proved to be more difficult to make. Initial operation of the cw beam was somewhat short-lived. After ~ h of cw operation, we lost vacuum in the HEBT line. Because the fiber-optic diagnostic units had not yet been delivered, we attempted to characterize the beam by installing a series of 0.25 mm-thick stainless steel foils transverse to the beampipe. From the size and shape of the holes melted in these foils, we could derive a crude estimate of the RFQ output emittance using the tomographic techniques.[5].

The 2-MeV melt contour of stainless steel corresponds to ~1.3 μA/cm^2, eight and one half standard deviations from the peak for a cw Gaussian 20-mA beam.

Extrapolation from these melt contours provided Gaussian beam profiles that were used to derive crude emittance values. From these emittances, it became clear immediately that there was a substantial difference between the predicted RFQ output emittance parameters and the crudely measured ones. This difference was responsible for the destruction of a vacuum seal and the subsequent loss of HEBT vacuum.

Following the delivery of the fiber-optic devices, we were able to derive much better values for the beam emittance than the foils allowed. Figures 4a and 4b show a comparison of the theoretical 95% beam fraction emittance (dashed lines) based on measured input beam and rf fields with the experimentally measured emittances (solid lines). The experimental beam matches the orientation of the theoretical beam quite well in the x-x' plane. However, we observe substantial differences in the y-y' plane. The initial beam transport in the HEBT was designed around the theoretical beam.
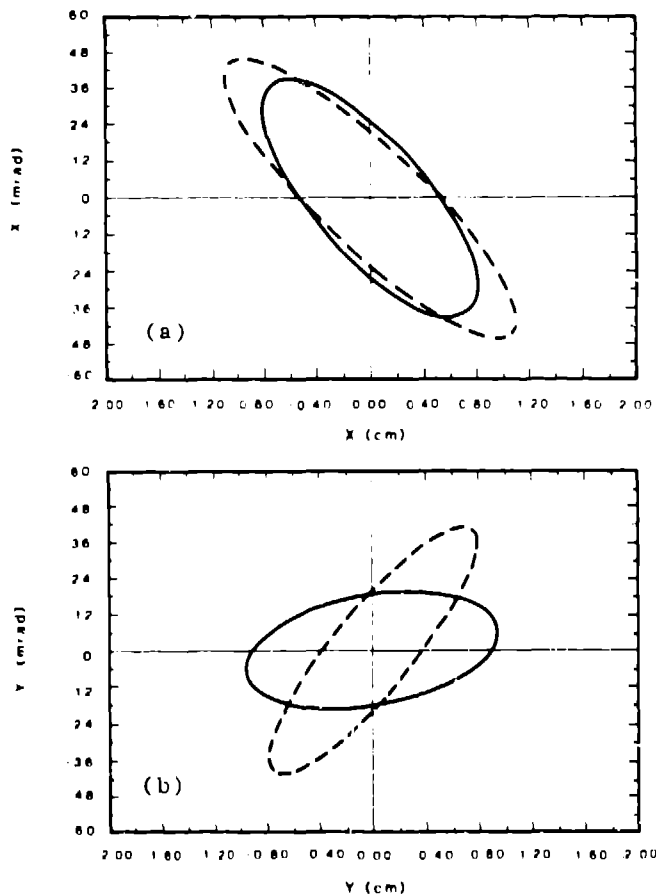
(a)

X (cm)

(b)

Y (cm)

Fig. 4. Comparison of measured x-x' and y-y' 95% beam fraction emittance ellipses with the theoretical predictions. The dashed ellipses show the expected beam emittances based on the measured injector beam and rf fields. The solid ellipses show the average x-x' and y-y' emittance values from several different measurements.

When the measured emittance profiles were used with the theoretical HEBT magnet settings in the beam-transport code TRACE,[*] the beam was predicted to intercept the beampipe at precisely the location where the vacuum seal melted. We therefore used TRACE to derive a new HEBT transport solution based on the measured profiles.

With this new transport solution, we were able to obtain preliminary measurements of many of the important parameters. Figure 5 shows the beam transmission as a function of rf drive power. The curve on the figure is drawn to guide the eye. Transmission was determined from the ratio of calorimetrically derived
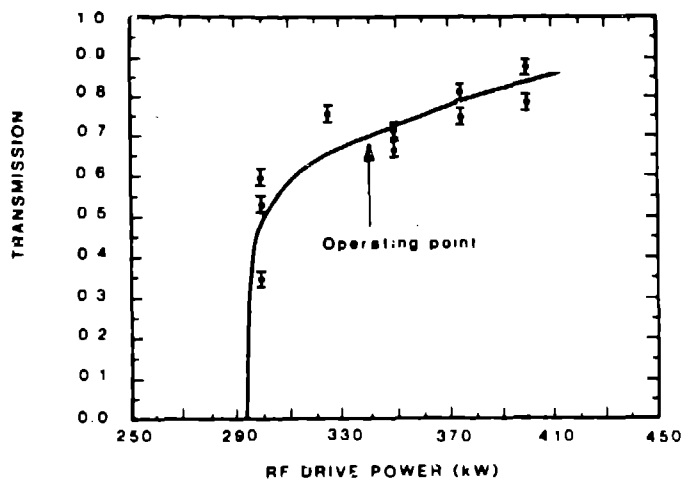
RF DRIVE POWER (kW)

Fig. 5. Beam transmission of the RFQ as a function of rf drive power with the current in the matching solenoid set to 510 A (see Fig. 6). The curved line is drawn simply to guide the eye.

LEBT and beamstop currents and is corrected for additional losses in the LEBT but not in the HEBT. Hence, these values are lower limits. Below 300 kW of rf power, the beam energy decreases rapidly, resulting in an increasing portion of the beam outside the energy acceptance of the HEBT. Hence, transmission measurements are unreliable and difficult to make

The minimum rf power needed to achieve the desired vane voltage in the RFQ was derived from Fig. 5. The 340-kW value compares favorably with the 325-kW estimate based on the measured Q and estimated copper losses.

Figure 6 shows beam transmission as a function of the final LEBT solenoid current, basically as a function of the phase-space match at the low-energy end of the RFQ. Contrary to expectations based on previous measurements made without the RFQ in place, the best transmission was obtained at 490 A of solenoid current. The expected best match was at 505 A. These transmission values are also somewhat lower than the expected 93% value.

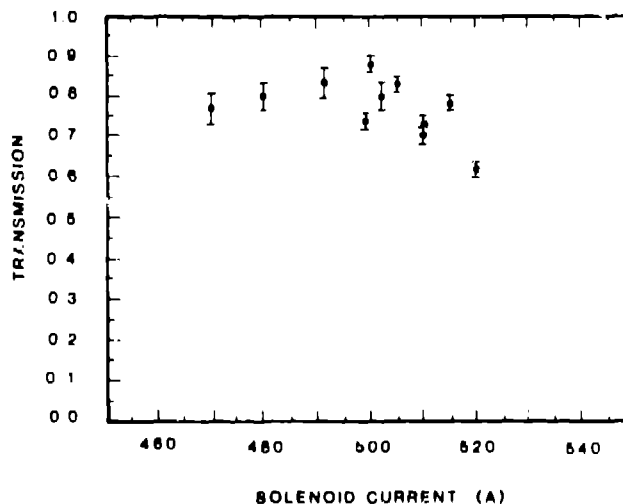SOLENOID CURRENT (A)

Fig. 6. Beam transmission of the RFQ as a function of current in the phase-space matching solenoid magnet.

To clear up these discrepancies, we digitized television camera frames from a viewport at the low-energy end of the RFQ. By using three successive scan lines from the digitized view, we could obtain beam profiles and, hence, an emittance reconstruction inside the RFQ

Extrapolation from these melt contours provided Gaussian beam profiles that were used to derive crude emittance values. From these emittances, it became clear immediately that there was a substantial difference between the predicted RFQ output emittance parameters and the crudely measured ones. This difference was responsible for the destruction of a vacuum seal and the subsequent loss of HEBT vacuum.

Following the delivery of the fiber-optic devices, we were able to derive much better values for the beam emittance than the foils allowed. Figures 4a and 4b show a comparison of the theoretical 95% beam fraction emittance (dashed lines) based on measured input beam and rf fields with the experimentally measured emittances (solid lines). The experimental beam matches the orientation of the theoretical beam quite well in the x-x' plane. However, we observe substantial differences in the y-y' plane. The initial beam transport in the HEBT was designed around the theoretical beam.
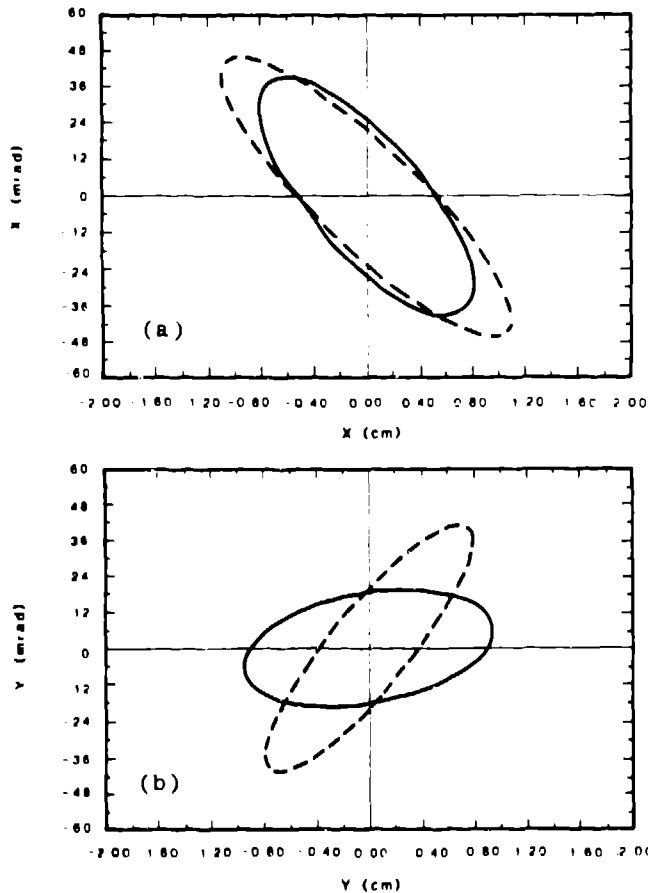

Fig. 4. Comparison of measured x-x' and y-y' 95% beam fraction emittance ellipses with the theoretical predictions. The dashed ellipses show the expected beam emittances based on the measured injector beam and rf fields. The solid ellipses show the average x-x' and y-y' emittance values from several different measurements.

When the measured emittance profiles were used with the theoretical HEBT magnet settings in the beam-transport code TRACE,[6] the beam was predicted to intercept the beampipe at precisely the location where the vacuum seal melted. We therefore used TRACE to derive a new HEBT transport solution based on the measured profiles.

With this new transport solution, we were able to obtain preliminary measurements of many of the important parameters. Figure 5 shows the beam transmission as a function of rf drive power. The curve on the figure is drawn to guide the eye. Transmission was determined from the ratio of calorimetrically derived
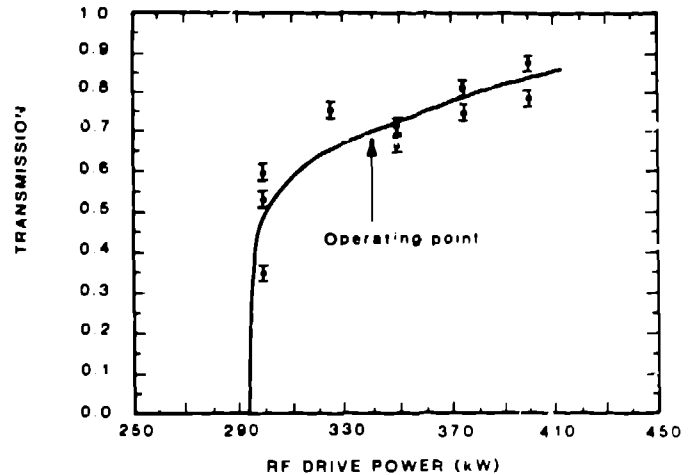

Fig. 5. Beam transmission of the RFQ as a function of rf drive power with the current in the matching solenoid set to 510 A (see Fig. 6). The curved line is drawn simply to guide the eye.

LEBT and beamstop currents and is corrected for additional losses in the LEBT but not in the HEBT. Hence, these values are lower limits. Below 300 kW of rf power, the beam energy decreases rapidly, resulting in an increasing portion of the beam outside the energy acceptance of the HEBT. Hence, transmission measurements are unreliable and difficult to make.

The minimum rf power needed to achieve the desired vane voltage in the RFQ was derived from Fig. 5. The 340-kW value compares favorably with the 325-kW estimate based on the measured Q and estimated copper losses.

Figure 6 shows beam transmission as a function of the final LEBT solenoid current, basically as a function of the phase-space match at the low-energy end of the RFQ. Contrary to expectations based on previous measurements made without the RFQ in place, the best transmission was obtained at 490 A of solenoid current. The expected best match was at 505 A. These transmission values are also somewhat lower than the expected 93% value.
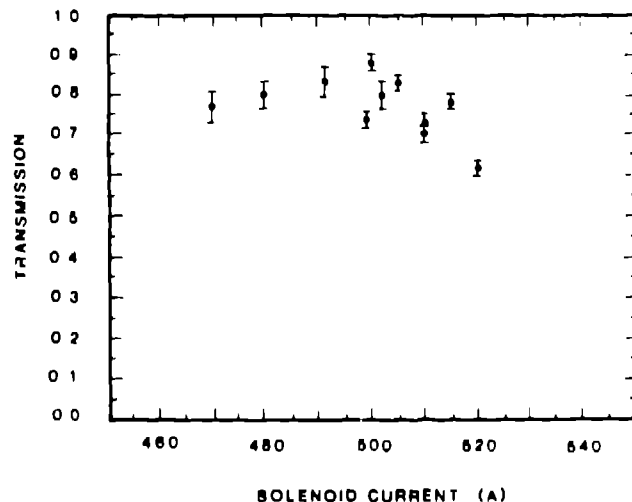

Fig. 6. Beam transmission of the RFQ as a function of current in the phase-space matching solenoid magnet.

To clear up these discrepancies, we digitized television camera frames from a viewport at the low-energy end of the RFQ. By using three successive scan lines from the digitized view, we could obtain beam profiles and, hence, an emittance reconstruction inside the RFQ

between the end wall and the vanes. These values are reliable to the extent that the space between the end wall and the vanes can be approximated by a drift.

We discovered that, at the same point, the experimentally determined emittance ellipse parameters alpha and beta were substantially different when the RFQ is in place than when those values were measured previously without the RFQ. In fact, the change in both parameters with increasing magnetic field actually changed sign--increasing with increasing magnetic field rather than decreasing as one would expect from a focusing system. Inspection of the RFQ end wall revealed that the stainless steel became magnetic sometime during fabrication and substantially distorts the magnetic field in this critical region. When the matching solenoid was moved 10 cm upstream from the RFQ end wall, the behavior of the emittance parameters returned to normal. The transmission peaked above 92% with the solenoid in this location. Excessive LEBT losses prevent satisfactory operation in this configuration.

Figures 7a and 7b show the measured unnormalized x-x' and y-y' emittances as a function of matching solenoid current. (These measurements were made before the discovery of the magnetic end wall.) The two sets of points in each figure represent the rms contour and the 95% beam-fraction contour. The error bars are representative of the reproducibility of the results for
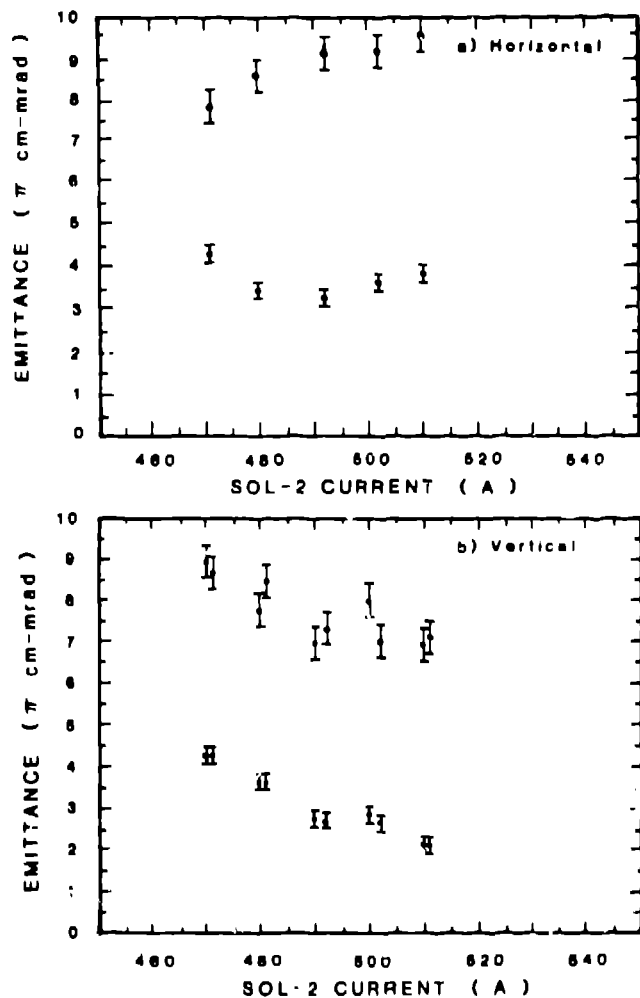
Fig. 7. RFQ output emittance as a function of current in the phase-space matching solenoid magnet. The upper points in each figure represent the unnormalized phase space area (divided by π) of the 95% beam fraction contour. The lower points represent the unnormalized phase-space areas of the rms contour. The error bars are representative of the reproducibility of the data using different data sets and different background subtraction methods.

different measurements and for different methods of subtracting the background (see Fig. 2). If we take average values for the x- and y-plane emittances and compare them with injector emittances, measured before transport through the LEBT the emittance growth in the RFQ is 3.925 ± 0.370, compared with the theoretical value of 2.7 (The 3.9 value should be taken as preliminary until better data are obtained). Many effects can be invoked to explain this value. Known aberrations in the 90° analyzing magnet and in the solenoids add to the effective emittance at the low-energy end. The previously mentioned magnetic distortion caused by the RFQ end wall also prevented a good phase-space match to the RFQ acceptance. Finally, breakup of H_2^+ ions through collisions with the residual gas in the system (about 3 μA/m at 20 mA) will add to the halo and will appear as emittance growth rather than beam loss because both beam and beam dissociation ions provide light from the ionization of residual gas atoms.

The dissociation ions could be eliminated by acceleration of a pure deuterium beam, but the radiation hazard would be extreme. In fact, even the 14 ppm of naturally occuring deuterium produces about 8 mR of neutrons at the beamstop with our 20-mA beam. We have distilled some deuterium-free hydrogen gas to eliminate this hazard for future operations.

During the collection of data for Fig. 5, we noted that between 375 and 400 kW of rf drive power, the output signal from the 80-MHz current transformer changed significantly. At lower power levels, the signal appeared to be an 80-MHz sine wave. However, above 375 kW of drive power this signal abruptly changed character. The calorimetrically derived beam current showed no change. Close examination of the beam profiles revealed no significant trend with rf power, but an abrupt change in beam position was noted in both x and y above 375 kW (Figs. 8a and 8b). With a dipole field component in the RFQ, one would expect a gradual shift of beam position with rf power rather than the abrupt shift seen in Fig. 8. We are investigating the possibility that saturation effects in the final-power rf amplifier may be responsible for this effect.

Without understanding all of these effects, we are reluctant to try to increase the beam current at this time, particularly in view of some more recent observations. The beam halo is slowly eroding the copper plating at one location inside the small-bore HEBT section. We have tried many different transport solutions that, according to TRACE, appear to be adequate. However, many of these solutions have caused melting problems. It does not appear that the core of the beam is causing the problems, but rather that the beam halo is responsible. The intensity of the halo is relatively small in comparison with the core of the beam, but is intense enough to cause problems by melting vacuum seals and, in some cases, aluminum and steel beampipes (remember that the 2-MeV melt contour of uncooled stainless steel is 1.3 μA/cm², 8.5 standard deviations for Gaussian beams). This halo continues to be the only major problem, particularly in the small-bore four-magnet section simulating the first drift tubes of the DTL. Without adequate measurements of the beam emittance profiles and their sensitivities to such parameters as injector matching, rf power, and beam steering, it is very difficult to determine an adequate beam tune for the HEBT. At the same time, it is equally difficult to measure these parameters without an adequate HEBT tune. After many repairs to the small-bore section, we have decided to temporarily replace this section with a larger bore transport system until we have adequately determined the RFQ output-beam characteristics and are confident that we can make this match without excessive risk.

a) Horizontal

POSITION/WIDTH (cm)

RF DRIVE POWER (kW)

b) Vertical

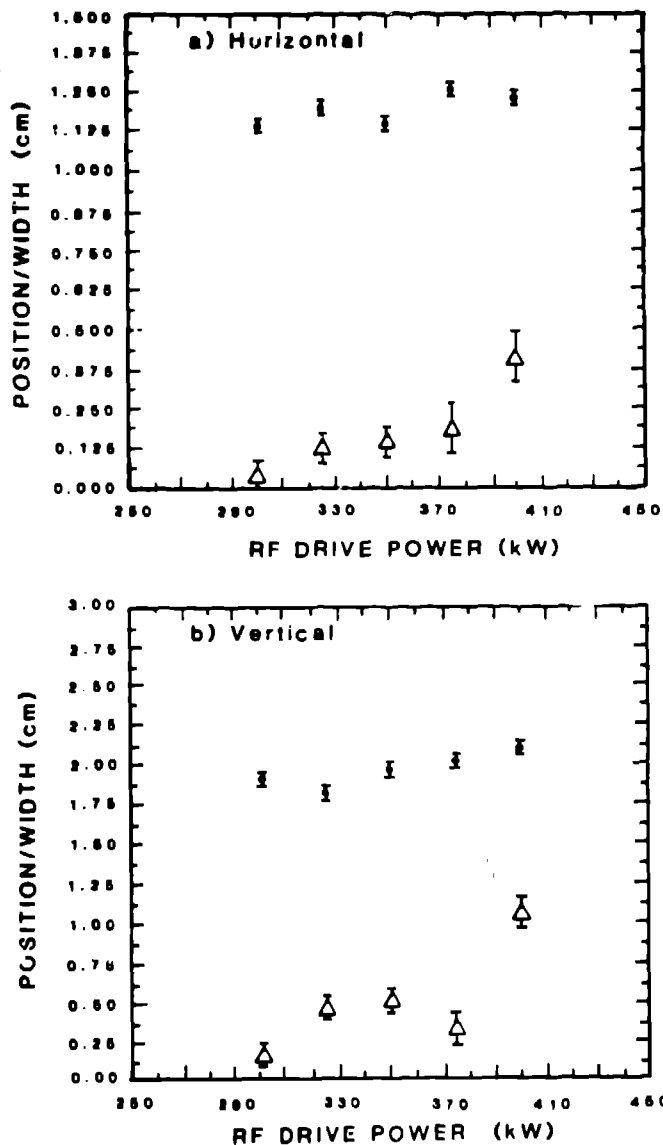POSITION/WIDTH (cm)

RF DRIVE POWER (kW)

Fig. 8. Comparison of the beam width (solid circles) and position (open triangles) as a function of the rf drive power. No obvious trend is evident in either the x- or y-beam widths. However, the beam abruptly shifts position when the rf drive power exceeds 375 kW.

Conclusions

Achieving cw rf operation was the most difficult task in the 2-MeV program and required some modest modifications to the RFQ design. However, now we have a reliable system that can be brought up to full cw operation within an hour. Initial characterization of the 2-MeV beam has revealed a major discrepancy between the expected output beam and the measured beam. None of the modifications made to the RFQ could have caused this effect. It is difficult to reconcile the fact that the x-x' phase space is close to that expected, whereas the y-y' phase space is not. This asymmetry has caused some difficulties in the transport of the 2-MeV beam, but we are taking steps to bring this under control.

The magnetic end wall of the RFQ seriously affects the matching of the beam into the RFQ and, hence, the transmission efficiency. We are investigating the best method, short of total replacement of the end wall, to circumvent this problem. By examination of Fig. 7, we see that the RFQ appears to act as a filter, transporting only that portion of the injected beam within the acceptance envelope of the device. This filtering

effect is why the output emittance is relatively independent of the input beam. Hence, asymmetries in the LEBT, either in beam emittance or aberrations, are washed out by the end of the RFQ. Therefore, it is difficult to find an explanation in the LEBT for the discrepancy in the output y-y' beam emittance. The only obvious asymmetry in the entire structure that could account for this difference is the interaction of the vane ends with the high-energy end wall. The opposing vanes that end in a peak (rather than a valley) have little additional effect from the exit aperture. The vanes that end in a valley, however, could interact with the exit aperture to form an additional half cell. This effect could be responsible for the additional focusing observed in the y-y' phase space, so that the output beams are no longer mirror images of each other. The asymmetric output emittance observed has a substantial impact on the matching into and subsequent acceleration by a DTL, and the source of this discrepancy must be identified.

As mentioned previously, the beam halo continues to be the only major problem. Temporary replacement of the DTL matching section with a larger bore beampipe will allow us to study the RFQ output beam more thoroughly without continuing to melt beampipes and vacuum seals. The sources of the halo are most likely from (a) an injector beam that is about 50% larger than the RFQ design value, (b) known aberrations in the analyzing magnet and solenoids, and (c) H_2^+ dissociation. Replacement of the ion source with one recently developed at Berkeley[9] would allow brighter beams to be produced. These beams would also use less of the solenoid aperture and, hence, would have less aberration-induced effective emittance growth. We have also discovered methods for reducing the inherent solenoid aberrations by shaping both the steel and the solenoid coils.[10]

None of these items can be completed within the time scale allowed by the present funding situation. Unless additional funding is forthcoming, we will be forced to shut down the program at the end of the fiscal year. We are pursuing a course of action that enables us to obtain as much information as possible before then. We feel it is imperative to reach the 100-mA goal before that time and to understand not only the source of the halo and of the emittance discrepancy, but to arrive at solutions for these problems as well.

References

1. M. D. Cornelius, "CW Operation of the FMIT RFQ Accelerator," Eighth Conference on the Application of Accelerators in Research and Industry, Nucl. Instr. & Meth., May 1985, to be published.

2. D. Ruzic, R. Moore, D. Manos, and S. Cohen, "Secondary Electron Yields of Carbon-coated and Polished Stainless Steel," J. Vac. Sci. Tech. 20 (1982), 1313.

3. M. D. Cornelius and R. J. Grieggs, "Elimination of Multipactoring in the FMIT RFQ Accelerator," Los Alamos National Laboratory report LAUR-84-2489, submitted to Nucl. Instr. & Meth.

4. T. D. Kirkendall, P. F. Varadi, and H. D. Doolittle, "Some Effects of Surface Layers on the Degassing Properties of Copper," J. Vac. Sci. Tech. 3 (1966), 214.

5. B. N. Minerbo, O. R. Sander, and R. A. Jameson, "Four Dimensional Beam Tomography," IEEE Trans. Nucl. Sci. 28 (3) (1981), 2231.

6. D. D. Chamberlin, J. S. Hollabaugh and C. J. Stump, Jr., "Imagescope to Photodiode Beam-Profile Imaging System," IEEE Trans. Nucl. Sci. 30 (4) (August 1983), 2201.

7. A. I. Brousseau and D. D. Chamberlin, "FMIT Direct-Current Beam Monitor," IEEE Trans. Nucl. Sci. 28 (3) (1981), 2209.

8. K. R. Crandall and D. P. Rusthoi, "TRACE: An Interactive Beam-Transport Code," Los Alamos National Laboratory report LA-10235-MS, January 1985.

9. K. W. Ehlers and K. N. Leung, "High Concentration H_2^+ or D_2^+ Ion Source," Rev. Sci. Instr. 54 (1983), 677.

10. D. D. Armstrong and J. D. Schneider, "Evaluation and Minimization of Aberrations for a Solenoid Lens," IEEE Trans. Nucl. Sci. NS-30 (4) (1983), 2793.